Single and High-Lift Airfoil Design Optimization Using Aerodynamic Sensitivity Analysis

Chang Sung Kim*, Byoungjoon Lee*, Chongam Kim and Oh-Hyun Rho****
Department of Aerospace Engineering
Seoul National University, Seoul, Korea 151-742

Abstract

Aerodynamic sensitivity analysis is performed for the Navier-Stokes equations coupled with two-equation turbulence models using a discrete adjoint method and a direct differentiation method respectively. Like the mean flow equations, the turbulence model equations are also hand-differentiated to accurately calculate the sensitivity derivatives of flow quantities with respect to design variables in turbulent viscous flows. The sensitivity codes are then compared with the flow solver in terms of solution accuracy, computing time and computer memory requirements. The sensitivity derivatives obtained from the sensitivity codes with different turbulence models are compared with each other. The capability of the present sensitivity codes to treat complex geometry is successfully demonstrated by analyzing the flows over multi-element airfoils on Chimera overlaid grid systems.

Key Word : sensitivity analysis, turbulence model, design variables, Chimera grid

Introduction

With the recent advances of computational power, design optimization methods using computational fluid dynamics (CFD) became popular tools in aerodynamic design. Before actual design process, an accurate and efficient flow solver is required for the computation of pressure distribution and aerodynamic loads such as lift, drag and pitching moment which are used in an objective function to be minimized. [1, 2] Derivatives with respect to each design variable may be obtained by the finite-difference method. It is, however, too expensive to compute the flow field iteratively with the incremented values of a design variable for complex two-dimensional or three-dimensional problems. In addition, this method is so sensitive to the step size of a design variable that it sometimes provides inaccurate signs or sensitivity derivatives. [3, 4] Therefore, more robust techniques have been proposed using the direct differentiation methods and the adjoint variable methods. [4-12] The direct differentiation methods provide computed derivatives which are coincident with finite-differenced derivatives,and are useful when the number of design variables is smaller than that of the objective function and constraints. On the other hand, the adjoint variable methods are more advantageous for their capabilitv to compute the gradients of the objective function and constraints when the number of design variables is larger than that of the objective function and constraints. The direct differentiation methods are dealt with the discrete form of the flow equations, and the adjoint variable methods adopt the formulation of the gradient in either a

* Research associate
** Professor
E-mail : chongam@plaza.snu.ac.kr, TEL : 02-880-1915, FAX : 02-887-2662

discrete or a continuous approach. In the discrete approach, which is used in the present work, the discretized governing equations are differentiated with respect to design variables while the adjoint equations are first differentiated and then discretized in the continuous approach. [9, 10]

In order to treat high Reynolds number flows accurately, it is necessary to incorporate the effect of turbulence in differentiating the governing equations. It is, however, very difficult to fully hand-differentiate the governing equations including the viscous terms and turbulence terms. Some software tools such as automatic differentiation [7, 8, 11] are used for the Navier-Stokes equations with a turbulence model. However, this approach is generally less efficient, in terms of computing time and computer memory, than hand-differentiation codes. [7, 12]

In the present work, the Navier-Stokes equations coupled with two-equation turbulence models are fully differentiated by hand. Among most popular two-equation turbulence models [13-16], the $k-\omega$ SST model proposed by Menter [15, 16] is mainly used and then compared with the $k-\omega$ model of Wilcox [13, 14], the standard $k-\varepsilon$ model [16]. Like the mean flow equations, the turbulence model equations are also hand-differentiated to accurately compute the sensitivity derivatives of flow quantities with respect to design variables in turbulent flows. Two codes, using a discrete adjoint method and a direct differentiation method respectively, are developed for the aerodynamic sensitivity analysis. The aerodynamic sensitivity analysis direct differentiation (ASADD) code and adjoint variable (ASAAV) code are then carefully validated for a turbulent flow over the RAE 2822 transonic airfoil. The derivatives from the sensitivity codes are compared with the finite-difference derivatives for non-geometric flow design variables and a geometric design variable. In order to demonstrate the capability to handle complex geometry in turbulent flows, sensitivity analysis codes using the Chimera grid scheme [17] are developed and validated for the flows over two- and three-element airfoils, the NLR 7301 airfoil with flap and the GAW-1 high-lift airfoil with a leading-edge slat and a trailing-edge flap.

Numerical Background

Flow Analysis

The governing equations are the two-dimensional, unsteady, compressible Navier-Stokes equations coupled with the $k-\omega$ SST turbulence model. [1] The governing equations are transformed in generalized coordinates and are solved with a finite-volume method. Using a backward Euler implicit method, the governing equations are discretized in time and linearized in delta form as

$$\left(\frac{I}{J\Delta t}+\left[\frac{\partial R}{\partial Q}\right]^n\right)\Delta Q=-R^n \tag{1}$$

where J is the Jacobian of transformation, R is the residual of the steady-state flow equations, and Q is the 6-element vector of conservative variables $(\rho, \rho u, \rho v, \rho e, \rho k, \rho\omega)^T$.

For the calculation of the residual, convective terms are upwind-differenced based on Roe's Flux Difference Splitting (FDS) scheme [18] and viscous terms are central-differenced. A MUSCL (Monotone Upstream Centered Scheme for Conservation Laws) approach using a third order interpolation is used to obtain a higher order of spatial accuracy. [19] The third order of spatial accuracy is kept in all calculations. For a temporal integration, Yoons LU-SGS scheme [20] is adopted to efficiently solve Eq. (1). Wall boundary conditions are applied explicitly with the non-slip condition. For inflow and outflow boundaries, characteristic conditions based on one-dimensional Riemann invariants are imposed. For the Chimera grid scheme, a bilinear

interpolation which is known to be robust and easy to implement is adopted for the hole-cutting boundary. [1]

Sensitivity Analysis

The discrete residual of steady-state flow equations R and objective function F are dependent on Q, X and D as

$$R=R(Q,X,D)=0,\quad F=F(Q,X,D) \tag{2}$$

where X is computational grid position and D is the vector of design variables. Introducing a Lagrangian multiplier yields the following equation.

$$\begin{aligned}\left\{\frac{dF}{dD}\right\}=&\left\{\frac{\partial F}{\partial Q}\right\}^T\left\{\frac{dQ}{dD}\right\}+\left\{\frac{\partial F}{\partial X}\right\}^T\left\{\frac{dX}{dD}\right\}+\left\{\frac{\partial F}{\partial D}\right\}\\&+\Lambda^T\left(\left[\frac{\partial R}{\partial Q}\right]\left\{\frac{dQ}{dD}\right\}+\left[\frac{\partial R}{\partial X}\right]\left\{\frac{dX}{dD}\right\}+\left\{\frac{\partial R}{\partial D}\right\}\right)\end{aligned} \tag{3}$$

Using a system of the following adjoint equations, the sensitivity derivatives of the objective function can be calculated as

$$\left\{\frac{dF}{dD}\right\}=\left\{\frac{\partial F}{\partial X}\right\}^T\left\{\frac{dX}{dD}\right\}+\left\{\frac{\partial F}{\partial D}\right\}+\Lambda^T\left(\left[\frac{\partial R}{\partial X}\right]\left\{\frac{dX}{dD}\right\}+\left\{\frac{\partial R}{\partial D}\right\}\right) \tag{4}$$

if and only if the arbitrary vector Λ satisfies the following equation.

$$\left[\frac{\partial R}{\partial Q}\right]^T\Lambda+\left\{\frac{\partial F}{\partial Q}\right\}=\{0\}^T \tag{5}$$

More details about the sensitivity analysis for Navier-Stokes equations with two-equation turbulence models, including boundary treatments for single-block and Chimera overlapping grids, are found in Ref. 2.

Results and Discussion

Effects of Turbulence Models

In order to study the effects of turbulence models, the sensitivity derivatives from the $k-\omega$ SST model are compared in Table 1 with those from the standard $k-\varepsilon$ and $k-\omega$ model at a Mach number of 0.73, a Reynolds number of 6.5 millions and an angle of attack 2.79 degrees. The sensitivity derivatives are computed for the lift coefficient with respect to angle of attack. For each turbulence model, the derivatives obtained from the adjoint variable (AV) code coincide with the direct differentiation (DD) results. Angle of attack α is given as a flow design variable and a geometric change is given on the upper airfoil surface using a Hicks-Henne function by

$$\begin{aligned}y&=y_o+\beta f(x)\\F(x)&=\sin^3(\pi x^{\ln 0.5/\ln 0.6})\end{aligned} \tag{6}$$

It is noted, however, that the $k-\omega$ model shows a noticeable difference with the other two models in case of geometric change β. This can be explained by that the shock position predicted by the $k-\omega$ model is different from the results of the other two models as shown in Fig. 1, and the geometric change is applied to the region where a strong shock wave develops. The effects of turbulence models on the prediction of aerodynamic load coefficients over single and multi-element airfoils were previously reported in Ref. 1.

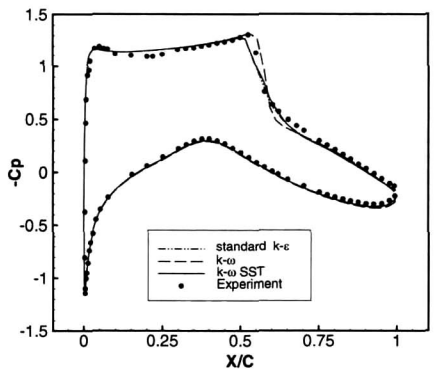

Fig. 1. Surface pressure coefficients over the RAE 2822 airfoil at AOA=2.79 deg, M=0.73, and Re=6.5 million.

Table 1. Effects of turbulence models on sensitivity derivatives.

	$\frac{\partial Cl}{\partial D}$	DD	AV
$k-\omega$ SST	α	8.7416	8.7416
	β	10.238	10.238
Standard $k-\varepsilon$	α	10.227	10.227
	β	7.7078	7.7078
$k-\omega$	α	8.9427	8.9427
	β	2.6211	2.6211

Sensitivity Analysis on Chimera Overlaid Grids

In order to treat complex geometry such as two- and three-element airfoils, aerodynamic sensitivity analyses are applied on Chimera grid systems using the DD code and the complete AV code using the $k-\omega$ SST model.

Two-Element Airfoil

In two-element airfoil case, the flow over the NLR7301 airfoil with a 32%c flap is tested at a Mach number of 0.3 and a Reynolds number of 3.0 million. The flap is positioned with a deflection angle of 20 degrees, an overlap of 5.3%c and a gap of 2.6%c. A 249x81 hyperbolic grid for the basic airfoil and a 125x41 grid for the flap are used for a Chimera grid system with the wall spacing on the order of 10^{-6} chord. The computed surface pressure coefficient using the $k-\omega$ SST model is compared with the experimental data [22] at a Mach number of 0.185, a Reynolds number of 2.51 million, and an angle of attack of 6.0 degrees in Fig.2. The sensitivity derivatives of lift coefficient with respect to the freestream Mach number, angle of attack, and geometric changes of the main airfoil and flap are presented in Table 2. For geometric changes of the main airfoil, the upper surface is deformed using Eq. (7) while both the upper and lower surfaces of the flap are changed using the following equation.

$$y = y_o + \beta f(x)$$
$$F(x) = \sin^3(\pi x^{\ln 0.5/\ln 0.4}) \tag{7}$$

where y_0 represents the original flap geometry and β is the design variable of concern.

Much like the case of single airfoil, the DD code shows quite a similar convergence with

the flow solver. In this case, the AV code requires about 5 times more computing time than the flow solver, while the DD code requires about 1.5 times. For the computer memory, the AV code requires about 2 times more memory than the flow solver, while the DD code requires about 1.6 times.

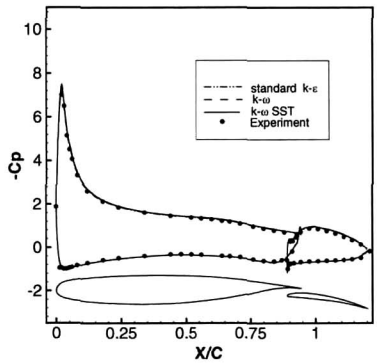

Fig. 2. Surface pressure coefficients over the NLR 7301 with flap.

Table 2. Sensitivity derivatives of lift for two-element airfoil.

$\frac{\partial Cl}{\partial D}$	DD	AV
M_∞	0.0810	0.0810
α	7.9886	7.9886
Main airfoil	1.7736	1.7736
Flap	-11.981	-11.981

Three-Element Airfoil

In three-element airfoil case, the flow over the NASA GAW-1 high-lift airfoil with a 15%c leading-edge slat and a 29%c trailing-edge flap is tested at an angle of attack of 2.0 degrees. The slat is positioned with a deflection angle of -42 degrees, an overlap of 1.5%c and a gap of 1.5%c, while the flap is positioned with a deflection angle of 30 degrees, an overlap of 0.0%c and a gap of 2.5%c. Figure 3 shows the computed surface pressure coefficients comparing with the experimental data [23] at a Mach number of 0.15, a Reynolds number of 0.65 million, and an angle of attack of 12.0 degrees.

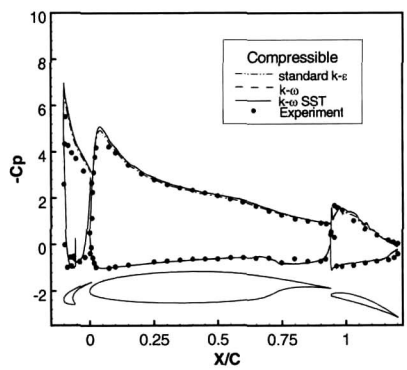

Fig. 3. Surface pressure coefficients over the GAW-1 high-lift airfoil.

Table 3. Sensitivity derivatives of lift for three-element airfoil.

$\frac{\partial Cl}{\partial D}$	DD	AV
M_∞	0.5218	0.5218
α	8.6889	8.6889
Main airfoil	1.7887	1.7887
Flap	-11.0918	-11.0918
Slat	-0.1643	-0.1643

The sensitivity derivatives of lift coefficient with respect to the freestream Mach number, angle of attack, and geometric changes of three elements are presented in Table 3. For the geometric change of the slat, both the upper and lower surfaces of the slat are changed using Eq. (6). As in two-element airfoil case, the consistency of the sensitivity derivatives from the AV and DD code on the Chimera grid can be confirmed.

Design Examples

In order to show the capability of both sensitivity analysis codes to obtain a desired optimal geometry, the adjoint variable (AV) code is used for single and multielement airfoil design optimization through the design procedure shown in Fig. 4. Optimization is performed using the Broydon-Fletcher-Goldfarb-Shanno (BFGS) variable metric method supported by the DOT commercial software. [24] Twenty geometric design variables are given on both upper and lower airfoil surfaces with ten Hicks-Henne functions on each surface.

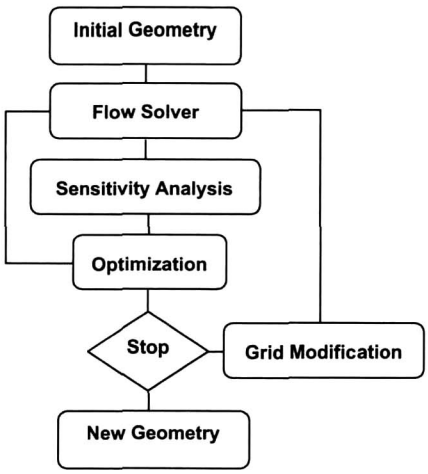

Fig. 4. Flow chart of numerical design optimization.

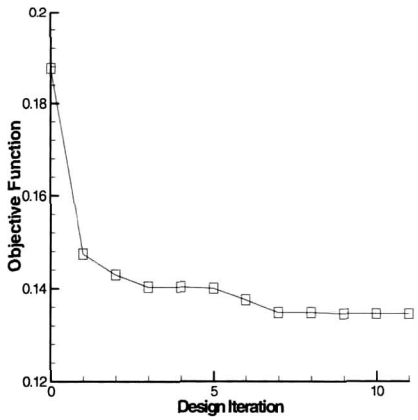

Fig. 5. Convergence of objective function in case of single airfoil design.

Single Airfoil Design

The objective in the first example is to reduce the drag coefficient over the RAE2822 airfoil with a fixed lift coefficient. The flow conditions are same with the sensitivity analysis case. Thus the objective function is given by

$$\text{Minimize} \quad F = w \times Cd + \max(Cl - Cl_0, 0.0) \tag{8}$$

where Cl_0 is initial lift coefficient and w is a weighting value of lift-to-drag ratio. After 11 design iterations, the drag coefficient is reduced from 0.01876 to 0.01345 while the lift coefficient is fixed at 0.7376 as shown in Fig. 5. This design example calls flow solver 47 times and sensitivity analysis code 11 times, respectively. The initial and design surface pressure coefficient distributions are shown in Fig. 6. The shock wave on the initial upper surface is disappeared on the final one.

Multielement Airfoil Design on Chimera Grid

The objective in this example is to maximize the lift coefficient over the NLR 7301 airfoil with flap. The flow conditions are same with the sensitivity analysis case. The objective function is given by

$$\text{Maximize} \quad F = Cl - w \times \max(Cd - Cd_0, 0.0) \tag{9}$$

where Cd_0 is initial lift coefficient and w is a weighting value of lift-to-drag ratio. Total 41 design variables including flap deflection angle are used. After 7 design iterations, the lift coefficient is increased from 2.5748 to 2.9403 while the drag coefficient is fixed at 0.03777. This design example calls flow solver 31 times and sensitivity analysis code 7 times, respectively. The initial and design surface pressure coefficient distributions are shown in Fig. 7.

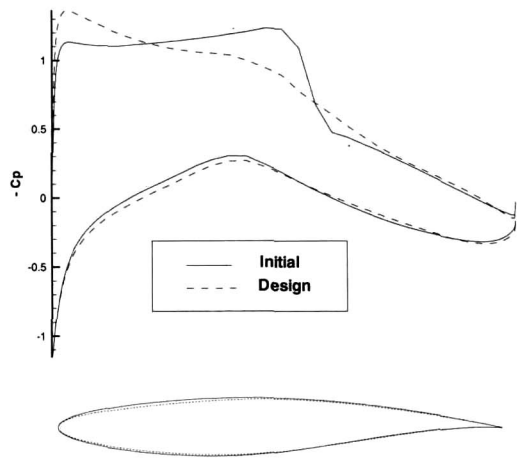

Fig. 6. Initial and design Cp distributions for single airfoil.

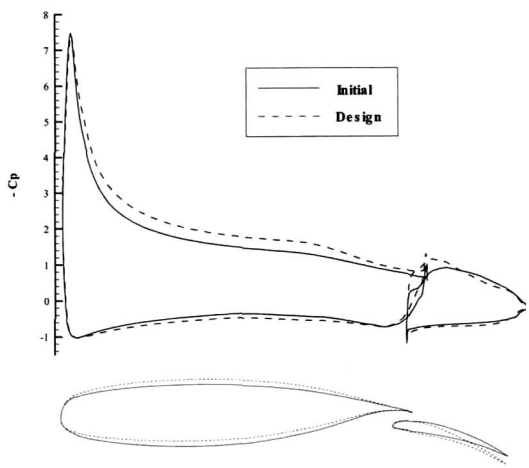

Fig. 7. Initial and design Cp distributions for multielement airfoil.

Conclusions

Aerodynamic sensitivity analysis using a direct differentiation method and an adjoint variable method were carried out for the Navier-Stokes equations coupled with two-equation turbulence models. Three two-equation turbulence models were adopted and differentiated by hand to obtain the sensitivity derivatives of aerodynamic objectives with respect to design variables in turbulent flows. Through numerous test cases, it was noted that the derivatives from the sensitivity codes are in consistency with each other. In addition, both sensitivity analysis codes using the Chimera grid scheme were developed and validated to treat complex geometry such as two- and three-element airfoils. For the AV code using the Chimera grid, careful treatments were required for the hole-cutting boundary. Both the ASADD and ASAAV code developed in the present work showed a good capability to obtain the accurate sensitivity derivatives of aerodynamic load coefficients with respect to design variables, and ASAAV code was successfully applied to single and multielement airfoil design examples.

Acknowledgement

This research was sponsored by the Brain Korea 21 Project.

References

1) Kim, C. S., Kim, C., and Rho, O. H., Parallel Computations of High-Lift Airfoil Flows Using Two-Equation Turbulence Models, *AIAA Journal*, Vol.38, No.8, August 2000, pp.

1360-1368.

2) Kim, C. S., Kim, C., and Rho, O. H., Sensitivity Analysis for the Navier-Stokes Equations with Two-Equation Turbulence Models, *AIAA Journal*, Vol.39. No.5, 2001, pp.838-845.

3) Eyi, S., and Lee, K. D., Effect of Sensitivity Calculation on Navier-Stokes Design Optimization, AIAA 94-0060, Jan. 1994.

4) Nielsen, E. J., and Anderson, W. K., Aerodynamic Design Optimization on Unstructured Meshes Using the Navier-Stokes Equations, AIAA 98-4809, Jan. 1998.

5) Eleshaky, M. E., and Baysal, O., Aerodynamic Shape Optimization Using Sensitivity Analysis on Viscous Flow Equations, Journal of Fluid Engineering, Vol.115, No.3, 1993, pp. 75-84.

6) Ajmani, K., and Taylor, A. C. III, Discrete Sensitivity Derivatives of the Navier-Stokes Equations with a Parallel Krylov Solver, AIAA 94-0091, Jan. 1994.

7) Sherman, L. L., Taylor, A. C. III, Green, L. L., Newman, P. A., Hou, G. J., and Korivi, V. M., First- and Second-Order Aerodynamic Sensitivity Derivatives via Automatic Differentiation with Incremental Iterative Methods, AIAA-94-4262-CP, Sep. 1994.

8) Mohammadi, B, Optimal shape Design, Reverse Mode of Automatic Differentiation and Turbulence, AIAA 97-0099, Jan. 1997.

9) Jameson, A., Pierce, N. A., and Martinelli, L., Optimum Aerodynamic Design Using the Navier-Stokes Equations, AIAA 97-0101, Jan. 1997.

10) Soemarwoto, B. I., The Variational Method for Aerodynamic Optimization Using the Navier-Stokes Equations, NASA/CR-97-206277, ICASE Report No. 97-71, Dec. 1997.

11) Taylor, A. C. III, and Osolo, A., Aerodynamic Design Sensitivities By Automatic Differentiation, AIAA 98-2536, June 1998.

12) Kim, H. J., Kim, C. A., Rho, O. H., and Lee, K. D., Aerodynamic Sensitivity Analysis For Navier-Stokes Equations, AIAA 99-0402, Jan. 1999.

13) Wilcox, D. C., Reassessment of the Scale-Determining Equation for Advanced Turbulence Models, *AIAA Journal*, Vol. 26, No. 11, 1988, pp. 1299-1310.

14) Wilcox, D. C., Simulation of Transition with a Two-Equation Turbulence Model, *AIAA Journal*, Vol. 32, No. 2, Feb. 1994, pp. 247-255.

15) Menter, F. R., Influence of Freestream Values on the $k-\omega$ Turbulence Model Predictions, *AIAA Journal*, Vol. 30, No. 6, August 1992, pp. 1651-1659.

16) Menter, F. R., Two-Equation Eddy-Viscosity turbulence Models for Engineering Applications, *AIAA Journal*, Vol. 32, No. 8, August 1994, pp. 1598-1605.

17) Steger, J. L., Doughty, F. C., and Beneck, J. A., A Chimera Grid Scheme, Advances in Grid Generation, FED, Vol. 5, ASME, Edited by Ghia, K. N., New York, 1983, pp. 59-69.

18) Roe, P. L., Approximate Riemann Solvers, Parameter Vectors and Difference Schemes, Journal of Computational Physics, Vol.43, 1981, pp.357-372.

19) Hwang, S. W., Numerical Analysis of Unsteady Supersonic Flow over Double Cavity, Ph.D. Dissertation, Seoul Natl Univ., Seoul, Korea, 1996.

20) Yoon, S., and Kwak, D., Three-Dimensional Incompressible Navier-Stokes Solver Using Lower-Upper Symmetric-Gauss-Seidel Algorithm, *AIAA Journal*, Vol. 29, June 1991, pp. 874-875.

21) Cook, P. H., McDonald, M. A., and Firmin, M. C. P., Aerofoil RAE 2822 Pressure Distributions, and Boundary Layer and Wake Measurements, AGARD AR 138, May 1979, A6-1 to A6-77.

22) Berg, B. v. d., Boundary Layer Measurements On a Two-Dimensional Wing With Flap, NLR TR 79009 U, Jan. 1979.

23) Braden, J. A., Whipkey, R. R., Jones, G. S., and Lilley, D. E., Experimental Study of the Separating Confluent Boundary-Layer, NASA Contractor Report 3655.

24) DOT Users Manual, Version 4.00, VMA Engineering, Vanderplaats, Miura & Associate, Inc., 1993.